Lisa M. Schwartz, Thomas R. Bukowski, James D. Ploger and James B. Bassingthwaighte
Am J Physiol Heart Circ Physiol 279:1502-1511, 2000.

You might find this additional information useful...

This article cites 44 articles, 17 of which you can access free at:
http://ajpheart.physiology.org/cgi/content/full/279/4/H1502#BIBL

This article has been cited by 3 other HighWire hosted articles:

GENTEX, a general multiscale model for in vivo tissue exchanges and intraorgan metabolism
J. B Bassingthwaighte, G. M Raymond, J. D Ploger, L. M Schwartz and T. R Bukowski
Phil Trans R Soc A, June 15, 2006; 364 (1843): 1423-1442.
[Abstract] [Full Text] [PDF]

Endothelial and Microvascular Function
D. Striimper, M. Durieux and P. Roekaerts
Seminars in Cardiothoracic and Vascular Anesthesia, September 1, 2003; 7 (3): 225-238.
[Abstract] [PDF]

Transient transcapillary exchange of water driven by osmotic forces in the heart
M. R. Kellen and J. B. Bassingthwaighte
Am J Physiol Heart Circ Physiol, August 7, 2003; 285 (3): H1317-H1331.
[Abstract] [Full Text] [PDF]

Medline items on this article's topics can be found at http://highwire.stanford.edu/lists/artbytopic.dtl on the following topics:

Biophysics .. Luminal Membranes
Biochemistry .. Interstitial Fluid
Cell Biology .. Endothelial Cells
Cell Biology .. Myocytes
Neuroscience .. Adenosine
Physiology .. Pigs

Updated information and services including high-resolution figures, can be found at:
http://ajpheart.physiology.org/cgi/content/full/279/4/H1502

Additional material and information about ***AJP - Heart and Circulatory Physiology*** can be found at:
http://www.the-aps.org/publications/ajpheart

This information is current as of June 13, 2009 .

AJP - Heart and Circulatory Physiology publishes original investigations on the physiology of the heart, blood vessels, and lymphatics, including experimental and theoretical studies of cardiovascular function at all levels of organization ranging from the intact animal to the cellular, subcellular, and molecular levels. It is published 12 times a year (monthly) by the American Physiological Society, 9650 Rockville Pike, Bethesda MD 20814-3991. Copyright © 2005 by the American Physiological Society. ISSN: 0363-6135, ESSN: 1522-1539. Visit our website at http://www.the-aps.org/.

Downloaded from ajpheart.physiology.org on June 13, 2009

Am J Physiol Heart Circ Physiol
279: H1502–H1511, 2000.

Endothelial adenosine transporter characterization in perfused guinea pig hearts

LISA M. SCHWARTZ, THOMAS R. BUKOWSKI, JAMES D. PLOGER, AND JAMES B. BASSINGTHWAIGHTE
Department of Bioengineering, University of Washington, Seattle, Washington 98195-7962

Received 29 November 1999; accepted in final form 27 March 2000

Schwartz, Lisa M., Thomas R. Bukowski, James D. Ploger, and James B. Bassingthwaighte. Endothelial adenosine transporter characterization in perfused guinea pig hearts. *Am J Physiol Heart Circ Physiol* 279: H1502–H1511, 2000.—Adenosine (Ado), a smooth muscle vasodilator and modulator of cardiac function, is taken up by many cell types via a saturable transporter, blockable by dipyridamole. To quantitate the influences of endothelial cells in governing the blood-tissue exchange of Ado and its concentration in the interstitial fluid, one must define the permeability-surface area products (*PS*) for Ado via passive transport through interendothelial gaps [PS_g(Ado)] and across the endothelial cell luminal membrane (PS_{ecl}) in their normal in vivo setting. With the use of the multiple-indicator dilution (MID) technique in Krebs-Ringer perfused, isolated guinea pig hearts (preserving endothelial myocyte geometry) and by separating Ado metabolites by HPLC, we found permeability-surface area products for an extracellular solute, sucrose, via passive transport through interendothelial gaps [PS_g(Suc)] to be 1.9 ± 0.6 ml·g^{-1}·min^{-1} (n = 16 MID curves in 4 hearts) and took PS_g(Ado) to be 1.2 times PS_g(Suc). MID curves were obtained with background nontracer Ado concentrations up to 800 μm, partially saturating the transporter and reducing its effective PS_{ecl} for Ado. The estimated maximum value for PS_{ecl} in the absence of background adenosine was 1.1 ± 0.1 ml·g^{-1}·min^{-1} [maximum rate of transporter conformational change to move the substrate from one side of the membrane to the other (maximal velocity; V_{max}) times surface area of 125 ± 11 nmol·g^{-1}·min^{-1}], and the Michaelis-Menten constant (K_m) was 114 ± 12 μM, where ± indicates 95% confidence limits. Physiologically, only high Ado release with hypoxia or ischemia will partially saturate the transporter.

purine nucleoside transport; endothelial cells; multiple-indicator dilution technique; Michaelis-Menten kinetics; vasoregulation; adenosine 5′-triphosphate; heart

FACILITATED DIFFUSION SYSTEMS for nucleosides across mammalian plasma membranes are saturable, nonconcentrative, reversible, and inhibitable by a variety of nucleoside and nonnucleoside drugs. Uptake into cells is thought to be the first step in the rapid removal of adenosine from the vicinity of its receptors on the extracellular surface of adenosine-responsive cells. Once inside cells, adenosine can be rapidly metabolized or incorporated into the nucleotide pool. Nucleosides are lost from the heart during conditions of increased stimulation or stress. Because the capacity for de novo synthesis of purines from nonpurine precursors is low (52), the heart maintains its supply of purine nucleotides by uptake from plasma. The nucleoside transport system is bidirectional, allowing adenosine release and stimulation of receptors on target cells (27, 42). Olsson and Pearson (30) provide a most comprehensive and thoughtful review of cardiac purine physiology.

Nucleoside uptake has been studied in cardiac muscle (2, 9, 19, 29, 31, 51), but the use of long incubation intervals, the absence of controls for passive flux estimations, and the potential for the adenosine kinase to be the actual rate-limiting step rather than the transporter all suggest that the total accumulation rates measured represented incorporation into nucleotide rather than transmembrane transport. The multiple-indicator dilution (MID) technique is a valuable method for obtaining information on rapid reaction or transfer rates in an intact, functioning organ and provides a means of analysis of membrane transport kinetics distinct from the rates of intracellular transformation (4, 6, 14). In this study, the focus is on the transporter conductance across the luminal surface of the cardiac capillary endothelial cells (PS_{ecl} = permeability-surface area product of the endothelial cell, luminal surface), distinguishing this from the transport through the interendothelial clefts [permeability-surface area product via passive transport through interendothelial gaps (PS_g)].

We obtained MID data on [^{3}H]adenosine and reference intravascular and extracellular solutes in isolated Krebs-Ringer perfused guinea pig hearts by use of pulse injection into the inflow and rapid sequential collection of samples from the outflow. Background perfusate concentrations of nontracer adenosine reduce the effective PS_{ecl} by competition for the binding site, as is the case for any saturable mechanism for transmembrane conductance. The relationship between the estimates of PS_{ecl} from the MID data and the levels of the varied background concentrations of aden-

Address for reprint requests and other correspondence: J. B. Bassingthwaighte, Dept. of Bioengineering, Box 357962, Univ. of Washington, Seattle, WA 98195-7962 (E-mail: jbb@bioeng.washington.edu).

The costs of publication of this article were defrayed in part by the payment of page charges. The article must therefore be hereby marked "*advertisement*" in accordance with 18 U.S.C. Section 1734 solely to indicate this fact.

0363-6135/00 $5.00 Copyright © 2000 the American Physiological Society

Downloaded from ajpheart.physiology.org on June 13, 2009

osine in each heart provides a measure of the affinity of the transporter for its adenosine ligand. Two partially independent methods of analysis were used to estimate the Michaelis-Menten constant (K_m) and the maximum rate of transporter conformational change to move the substrate from one side of the membrane to the other (maximal velocity; V_{max}).

METHODS

Isolated heart preparation. Adult guinea pigs (400–550 g) were heparinized and anesthetized with pentobarbital sodium (50 mg/kg ip), and their hearts were rapidly excised and Langendorff-perfused with modified Krebs-Ringer-bicarbonate buffer (KRB; see Ref. 28) including human serum albumin (0.1 mg/ml) and D-glucose (10 mM). A side-hole catheter was inserted though the apex of the right ventricle and secured in the pulmonary artery at a point ~5 cm above the base of the heart for outflow collection from the coronary sinus, right atrium, and right ventricle. Having an open-ended cannula allowed for rapid right ventricular outflow of air and fluid so that there was minimal delay volume in the heart and, therefore, minimal effective mixing volume in the right ventricle. The left ventricle was vented by use of a small catheter inserted through the apex to prevent fluctuations in ventricular pressure development that would result from accumulation of leakage through the aortic valve and Thebesian drainage.

The perfusion system consisted of five 2-l flasks surrounded by water at 41°C, with a 500-mm Allihn condenser attached to the mouth of each flask by a silicon stopper. During the experiment, each of the flasks contained KRB supplemented with unlabeled adenosine concentrations ranging from 0 to 1,000 μM. A transport blocker [either 5 μM nitrobenzylthioinosine (NBTI; Sigma Chemical) or 20 μM dipyridamole (Persantin; gift from Boehringer Ingelheim Pharmaceuticals)] was used as a final intervention in three studies. Perfusate was pumped from the bottom of the flask to the top of the condenser and returned to the flask as a thin film on the inside of the condenser. Filtered and humidified 95% O_2-5% CO_2 was introduced over the surface of the perfusate in the flask, flowed up the condenser, and exited the top via a small tube inserted through the silicon stopper. The perfusate flowed out of the bottom of the flasks through a distribution valve and was pumped through 8-μm filters, an in-line heat exchanger, a water-jacketed windkessel, and into the heart. The perfusion rate was controlled with a roller pump on the inflow line, and perfusion pressure and heart rate were measured with a transducer on the arterial cannula. Perfusate temperature in the heart was 37°C. Hearts were electrically paced at 300 beats/min. The preparation was allowed to stabilize for 20 min before the start of the experiment to allow for washout of blood and to enable the heart to adjust to blood-free perfusion.

Experimental protocol. The single-pass MID technique was used to quantify the capillary extraction of adenosine. Bassingthwaighte and Goresky (4) provide an overview of the approach. ^{131}I-labeled albumin was used as the intravascular reference tracer to provide a direct measure of the dispersion and delay in the arterial, capillary, and venous portions of the vascular bed. Bovine serum albumin (Sigma) was iodinated using chloramine T (Sigma) and sodium thiosulfate (Sigma) as described by McConahey and Dixon (26). The reaction mixture was immediately chromatographed on a 3.9 mm × 30 cm column equilibrated with NaH_2PO_4 (pH 7.5), and fractions corresponding to peak activity were collected. One milliliter of the collected eluent was dialyzed overnight at 4°C against 1 liter of KRB and vacuum filtered (0.2 μm) to remove free ^{131}I and any aggregates of the albumin.

Use of [U-^{14}C]sucrose (NEN Products) allowed evaluation of the additional process of permeation of the capillary wall via extracellular pathways and distribution in interstitial fluid (ISF) volume.

Aliquots of [2-^{3}H]adenosine (Amersham) were purified on HPLC <72 h before experimental use, dried, frozen, and redissolved in KRB on the day of the experiment. Contaminants in the form of uric acid, xanthine, hypoxanthine, and inosine constituted <2% of dose injections. No corrections were made in the calculation of metabolite recovery for the presence of these dose contaminants.

Indicator dilution curves were obtained by injecting a bolus (0.1 ml KRB containing ~4 μCi albumin, 1 μCi sucrose, and 4 μCi adenosine) into the aortic root. The timing of the injection, lasting 0.5–1.0 s, was recorded, and the midpoint was used as zero time ($t = 0$). Immediately before this injection, collection of coronary sinus outflow samples from the right ventricle into 60 ice-cold, tared test tubes at 1-s sampling intervals was begun. Thirty samples were collected at 1-s intervals and then another 30 at 2-s intervals. Each tube contained 250 μl of "stop solution," composed of 32 μM dipyridamole and 3 μM erythro-9-(2-hydroxy-3-nonyl)adenine hydrochloric acid (Burroughs Wellcome), to prevent the cellular uptake and deamination of adenosine by any remaining red blood cells. Control experiments verified that this solution prevented any disappearance of adenosine from the collected effluent samples.

To ensure that the heart was vasodilated throughout the entire series of injections, the first perfusate was chosen to have a background concentration above 10 μM adenosine. To keep adenosine concentrations within the cells and interstitium as low as possible, injections were made immediately after the time determined to be necessary to clear the tubing dead volume. After each test situation, the perfusate was switched to one containing zero adenosine to prevent accumulation of extravascular adenosine. Within several seconds, the adenosine concentrations in the outflow were very nearly as high as the inflow concentrations; the outflow values were used as the intracapillary concentration, although they will be slightly lower than the true average.

Radioactive microspheres (^{85}Sr, 15 μm; NEN Products) were injected into the aortic root at the end of each experiment to assess flow heterogeneity in the myocardium. Each injectate contained a volume of 50–100 μl and an activity of ~2 μCi. At the end of each experiment, the wet weight of the myocardium, devoid of fatty tissue, was measured. Hearts were then sectioned into 36 pieces, ranging in weight between 0.01 and 0.20 g, which were counted for 10 min by use of a multichannel well-type gamma-counter. Deposition densities of the microspheres were used to measure the probability-density function of regional myocardial blood flows as described by Gonzalez and Bassingthwaighte (13) and Bassingthwaighte et al. (5); these distribution functions define the flow heterogeneity used for the analysis of the MID data. Over 100,000 spheres were injected, giving over 3,000 spheres per piece on average; the microsphere error in this situation is a standard deviation (SD) of <5% (39).

Sample processing. Outflow samples were shaken immediately after collection to mix the stop solution and effluent. Each sample was then weighed, and a 100-μl aliquot was placed into a tube counting ^{131}I for 10 min. Samples were kept ice-cold throughout this processing. The remainder of the sample was frozen for separation of nucleosides by use of HPLC techniques. Duplicates of three dilutions of each in-

Downloaded from ajpheart.physiology.org on June 13, 2009

jected dose were made in collected effluent and processed identically.

Hundred-microliter aliquots of collected samples and doses were assayed on a Waters HPLC system with the use of a 25-min isocratic method and a C-18 stainless steel column (μBondapak, 30 cm × 3.9 mm; Waters) at a flow rate of 1 ml/min (16). The mobile phase consisted of 10 mM $NH_4H_2PO_4$ (pH 5.5) and 100% methanol (10:1 vol/vol). The eluted fractions corresponding to adenosine, inosine, hypoxanthine + xanthine, and sucrose were collected and added to scintillation cocktail for 10 min of beta-counting (Beckman Instruments, LS-5800). Corrections were made for counting efficiency. Tracer recoveries using these methods were >95%.

Nontracer adenosine concentrations in the perfusate at the time of injection were determined by quantitating the concentrations in the first collected effluent tube taken before the injection of the tracer bolus for each experiment. Concentrated samples were analyzed by use of a 20-min linear gradient method as described by Manfredi and Sparks (25). Hundred-microliter samples were injected onto a reverse-phase and C-18 stainless steel column (μBondapak, 30 cm × 3.9 mm; Waters). The gradient was produced with the use of two solvent reservoirs, starting with 100% 4 mM KH_2PO_4 (pH 4.5) and going to 40% methanol-water (70:30) over 20 min. The presence and quantitation of adenosine in samples were determined by comparison of retention times, peak height, and area on sample chromatograms with those obtained from standards. Sensitivity with this method was in the range of 2 nmol. Because we collected ~20 ml of effluent perfusate for the background sample, evaporated to dryness and resuspended in 200 μl, the lowest levels measurable were >10 nM, but our lowest levels were ~0.1 μM in these experiments.

Data analysis. Each dilution curve was normalized with respect to injected activity and expressed as the fraction of injected tracer emerging in the outflow per second [$h(t)$]. For a given tracer

$$h(t_i) = F_p \cdot C(t_i)/q_0 \quad (1)$$

where $h(t_i)$ is the fraction of dose exiting per second, t_i is the midpoint of the sampling period, F_p is the flow of perfusate in milliliters per second, $C(t_i)$ is the counts per minute per milliliter of effluent for *sample i,* and q_0 is the counts per minute of the injected dose. The area of the outflow dilution curve and the mean transit time through the heart for each tracer were calculated from each of the normalized $h(t)$ curves. Instantaneous extractions of sucrose and adenosine were calculated by use of the formula

$$E(t) = 1 - h_D(t)/h_R(t) \quad (2)$$

where $E(t)$ is the instantaneous extraction at time t, $h_D(t)$ is the fraction of injected diffusible or permeating tracer exiting per unit of time, and $h_R(t)$ is the similar value for the intravascular reference tracer, albumin. E_{max} is the maximum of $E(t)$ after smoothing, as defined by Guller et al. (15), and occurs during the upslope toward the peak of $h_R(t)$.

The indicator dilution curves were analyzed in light of the expectation that sucrose escapes from the plasma region only through interendothelial clefts, whereas adenosine traverses both the clefts and the luminal plasmalemma of the endothelial cells (6, 14). Although we might have used a model of a set of parallel capillary-tissue units to account for the distribution of regional myocardial flows observed with microspheres (22), we chose to use a single-capillary analysis because the errors in doing so are small when back diffusion from the interstitium to the plasma is small (21) (*assumption 1*). The value of PS_g for sucrose [PS_g(Suc)] was obtained by the Crone-Renkin expression, $PS_g(\text{Suc}) = -F \cdot \log_e[1 - E_{max}(\text{Suc})]$, where E_{max}(Suc) is the E_{max} for sucrose; then PS_g for adenosine [PS_g(Ado)] was fixed at $\beta \times PS_g$(Suc), where β, the expected ratio of permeabilities through the interendothelial clefts, should be equal to the ratio of free aqueous diffusion coefficients in the absence of significantly different steric hindrances in the interendothelial clefts. In the APPENDIX we provide analyses leading to the conclusion that the value of the ratio $\beta = PS_g(\text{Ado})/PS_g(\text{Suc}) = 1.20$ (*assumption 2*).

Analysis of transport kinetics. Facilitated transport via a transporter with a single binding site and *cis/trans* symmetry gives the same flux-to-concentration relationship as Michaelis-Menten enzyme kinetics (49). For indicator dilution studies, estimates of permeability-surface area products, the *PS* obtained from modeling analysis of indicator dilution curves for tracers, depends on the concentration of nontracer mother substance

$$PS_{ecl} = V_{max} \cdot S/(K_m + C_{Ado}) \quad (3)$$

where V_{max} (in $\mu M \cdot cm \cdot min^{-1}$; or, alternatively, in $nmol \cdot cm^{-2} \cdot min^{-1}$) represents the maximum rate of transporter conformational change to move the substrate from one side of the membrane to the other times the number of transporters per unit surface area available at the luminal surface, S is the surface area of the capillary wall (taken to be 500 cm^2/g tissue), K_m (in μM) is the equilibrium dissociation constant for the binding of substrate to the transporter and is the concentration of adenosine giving 50% saturation of the transporter sites, and C_{Ado} (in μM) is the background perfusate concentration of adenosine. Here we further assume that the association-dissociation processes are fast compared with the transmembrane translation (*assumption 3*).

Translated into molecular terms, V_{max} equals the concentration of transporter available to bind substrate at the external surface of the membrane multiplied by its rate of conformational change (the permeation event) when complexed with substrate, P_{TS} cm/min). When the total transporter concentration is T (in μM), the concentration at one face is T/2 for a transporter equally likely to face either side. This is the case when the T-S complex and the uncomplexed T have the same rates of conformational change to shift the active site from one side of the membrane to the other. In this symmetrical case, $V_{max} = P_{TS}$ T/2 (in $nmol \cdot min^{-1} \cdot cm^{-2}$), and $V_{max}S$ has the units $nmol \cdot min^{-1} \cdot g^{-1}$. Units for $V_{max}S/K_m$ can therefore be determined ($ml \cdot min^{-1} \cdot g^{-1}$), the same as for *PS*. We estimated values for $V_{max}S$, and, by assuming a capillary surface area of 500 cm^2/g (7), we obtained values for $V_{max} = PS_{ecl\ max} \cdot K_m/S$, where (from *Eq. 3*) $PS_{ecl\ max}$ is the value for PS_{ecl} when C_{Ado} is zero.

The estimates of PS_{ecl} for adenosine from the individual MID curves from the E_{max} values for sucrose and adenosine [E_{max}(Suc) and E_{max}(Ado), respectively] were obtained by taking into account that the total apparent permeability-surface area product for adenosine [PS_T(Ado)] has two components, transmembrane transport and cleft permeation

$$\begin{aligned} PS_{ecl} &= PS_T(\text{Ado}) - PS_g(\text{Ado}) \\ &= PS_T(\text{Ado}) - \beta \cdot PS_g(\text{Suc}) \\ &= -F \cdot \{\log_e[1 - E_{max}(\text{Ado})] - \beta \cdot \log_e[1 - E_{max}(\text{Suc})]\} \end{aligned} \quad (4)$$

and then fitting the set of values for PS_{ecl} from all of the curves with the Michaelis-Menten expression (*Eq. 3*) to get K_m and V_{max}. This is a variant of the Crone (11) method and assumes the absence of back flux of either adenosine or

Downloaded from ajpheart.physiology.org on June 13, 2009

sucrose from the ISF as well as the estimation of PS_g for adenosine as being β times that of sucrose, independent of concentration, which is appropriate for a passive flux, as in the APPENDIX. A corollary to *assumption 1* (that single capillary analysis is adequate) is that the ratio of PS_{ecl} to flow F is the same in all regions. An analysis in the style of Wangler et al. (50) using a four-region capillary-tissue exchange was not undertaken here.

The SENSOP optimization routine (10) was used to fit *Eq. 3* to the set of estimates of PS_{ecl} and to give measures of goodness of fit and estimates of confidence limits for K_m and V_{max}. Such a nonlinear optimization routine is preferred over linearization/graphical methods such as Lineweaver-Burke plots because the appropriate weighting of the observations relative to the originally observed data is better maintained.

RESULTS

Outflow dilution data. Twenty-one sets of indicator dilution curves were obtained from experiments in four isolated guinea pig hearts. Experimental conditions are listed in Table 1. The last digit of the experiment number is the sequence number for the particular heart. Mean perfusion pressure at the time of injection was 41 ± 4.8 mmHg under these vasodilated conditions. Perfusate flows averaged 7.4 ± 2.1 $ml \cdot min^{-1} \cdot g^{-1}$.

Tracer adenosine recoveries ranged from 62 ± 16% in the absence of competitors and blockers to 99 ± 2% in the presence of transport blockers. Monoexponential extrapolation of the tails of the curves gave <0.1% additional tracer for albumin, 1.0% for sucrose, and 0.2% for adenosine, and although these are underestimates, because we know the tails to be multiexponential (3), the incomplete recovery cannot be due to the short collection period. The similar recoveries of the nonmetabolized tracers, albumin and sucrose, indicate that the majority of tracer loss occurred during sample collection, which would affect all tracers equally and creates a small error in absolute, but not relative, scaling and does not influence parameter estimation. However, small additional errors may have occurred during sample preparation for HPLC analysis. Consequently, the areas of nonmetabolized albumin and sucrose curves, with tail extrapolation, were scaled to 1.0 for analysis to satisfy the conservation of mass requirements of the model. To preserve the relationship between the diffusible curves, the adenosine and sucrose curves were always scaled by the same factor.

Saturation studies. The normalized outflow dilution curves obtained from a series of four injections made within the same heart with varied concentrations of unlabeled adenosine in the perfusate are shown in Fig. 1. These curves possess features consistently found in the entire set of experiments.

Albumin, an unextracted intravascular reference tracer, has a relatively narrow high peak and more rapid decline than tracers that permeate the capillary membrane and then have a return flux that broadens the peak and extends the tail. Sucrose, an extracellular marker, diffuses into the ISF via the clefts between the endothelial cells. Its escape into the ISF is reflected in the peak

Table 1. *Experimental conditions and data summary*

Experiment No.	F_p, $ml \cdot min^{-1} \cdot g^{-1}$	C_{Ado}, μM	Pressure, mmHg	Recovery*			E_{max}†	
				Adenosine	Inosine	Hypo+Xan	Sucrose	Adenosine
			Saturation studies					
1101894	9.38	0.12	41	0.69	0.04	0.01	0.21	0.34
1901894	8.77	0.14	47	0.64	0.04	0.01	0.25	0.38
2107881	4.61	4.0	38	0.53			0.32	0.50
2107885	4.71	7.9	35	0.55	0.25	0.03	0.32	0.49
2107882	4.23	21	35	0.56			0.31	0.47
1901891	9.04	32	46	0.76	0.16	0.01	0.20	0.30
1101891	9.17	50	45	0.71	0.26	0.02	0.28	0.38
2107883	4.52	60	35	0.65			0.29	0.43
1101892	9.28	90	40	0.76	0.21	0.01	0.25	0.35
1901892	9.04	119	44	0.83	0.15	0.01	0.20	0.28
2909885	7.46	160	40	0.82	0.14		0.14	0.22
2909883	7.76	250	40	0.85	0.15		0.17	0.23
1101893	9.38	256	35	0.86	0.13	0.01	0.23	0.30
2909884	7.47	500	40	0.90	0.10		0.14	0.19
1901893	8.68	545	47	0.92	0.09	0.01	0.18	0.23
2107884	4.57	840	35	0.88			0.34	0.41

Experiment No.	F_p, $ml \cdot min^{-1} \cdot g^{-1}$	Inhibitor	Pressure, mmHg	Recovery			E_{max}	
				Adenosine	Inosine	Hypo+Xan	Sucrose	Adenosine
			Blocker studies					
2107886	4.81	dipyridamole	35	1.01	0.01	0	0.29	0.32
1101895	9.22	NBTI	46	0.99	0	0	0.30	0.34
1901895	8.64	NBTI	47	0.98	0	0	0.19	0.23

Experimental conditions and data summary. F_p, flow of perfusate; C_{Ado}, the background perfusate concentration of adenosine; Hypo, hypoxanthine; Xan, xanthine; E_{max}, maximum extraction; NBTI, nitrobenzylthioinosine. *Recoveries were scaled as described in RESULTS. †Extractions are based on scaled recoveries.

Downloaded from ajpheart.physiology.org on June 13, 2009

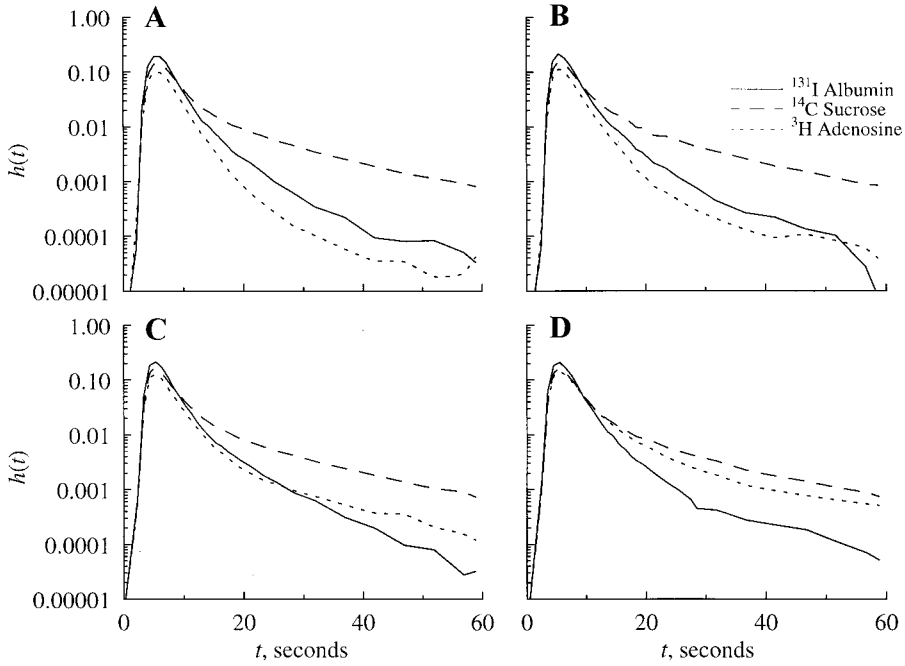

Fig. 1. Saturation of cellular tracer uptake with increasing background concentrations of nontracer adenosine. Successive panels are normalized outflow dilution curves obtained from the coronary sinus during perfusion with Krebs-Ringer-bicarbonate buffer (KRB) containing 4 (*A*; *experiment 2107881*), 21 (*B*; *experiment 2107882*), 60 (*C*; *experiment 2107883*), and 840 μM adenosine (*D*; *experiment 2107884*). Background unlabeled adenosine concentrations were determined from quantitation of first collected samples before the injection of the tracer-containing bolus. *t*, Time; *h*(*t*), the fraction of injected tracer emerging in the outflow per second.

height of the sucrose curve being lower than that of albumin. Because sucrose is not metabolized, it refluxes from the interstitium, and its curve crosses over the albumin curve 3–5 s after the peak. From its maximal extractions, E_{max} in Table 1, PS_g(Suc), which is $-F \log(1 - E_{max})$, averaged 1.94 ± 0.6 ml·g^{-1}·min^{-1}.

Adenosine is more extracted than sucrose, as seen from the lower peak concentrations of the adenosine curve than that of sucrose. Because the early parts of the curve, the upslope and peak, are governed primarily by the capillary barrier, the excess extraction of adenosine over sucrose represents a combination of its higher cleft permeability and its endothelial uptake. The cleft *PS* inferred from the sucrose data is critical to separating the two factors. Because adenosine is rapidly metabolized within cells, the area under the adenosine outflow curve is less than unity, and the curve does not cross over the sucrose curve even at high background adenosine levels.

As shown in Fig. 1, the shape of the dilution curves changed considerably with the addition of unlabeled adenosine to the perfusate. The stability of the preparation is demonstrated by the reproducibility of the albumin and sucrose curves. However, as the background adenosine concentration increased, the adenosine and sucrose curves became more alike. Because the two molecules have different diffusion coefficients and would therefore be expected to permeate the gaps somewhat differently, the curves would not be expected to completely overlap even in the event of total carrier saturability. However, if the carrier were saturated at the highest dose shown here, the adenosine curve would have crossed over the sucrose curve after the peak, reflecting its higher permeability and enhanced rate of escape from the interstitial space. That this did not happen means that there is either still some cellular uptake and retention or metabolism of the tracer adenosine. The analysis of the metabolic products of adenosine indicate that both play a role (Table 1). Maximum tracer adenosine recovery at high background nontracer levels was 92%, and HPLC analysis demonstrated that there was, even at 840 μM adenosine, some deamination to inosine and further degradation to hypoxanthine, xanthine, and uric acid. As will be seen, this concentration is still <10 times the estimated K_m for the transporter, so an uptake of several percent is to be expected.

Maximal inosine formation from injected tracer adenosine and release occurs at moderate background adenosine concentrations. Only 4% of tracer adenosine was recovered as inosine at unlabeled adenosine concentrations <0.2 μM, probably because the rate of incorporation of adenosine into the nucleotide pool was greater than the rate of deamination. However, at nontracer adenosine levels of 8 μM and greater, greater fractions of adenosine are deaminated to inosine, showing that at these extracellular levels the intracellular concentrations are also so high that adenosine kinase is saturated. At very high levels of nontracer adenosine, inosine release decreases. This may be due to saturation of adenosine deaminase or saturation of the nucleoside carrier. These effects should be quantifiable through model analysis describing all of the metabolic reactions, but this is beyond the scope of this study.

Effects of transport blockers. Normalized outflow dilution curves obtained during perfusion with KRB containing a blocker of the nucleoside transporter, dipyridamole or NBTI, are shown in Fig. 2. In neither case do the sucrose and adenosine curves truly overlap, indicating dissimilar permeabilities. In the absence of a functioning transport system across cell membranes,

Downloaded from ajpheart.physiology.org on June 13, 2009

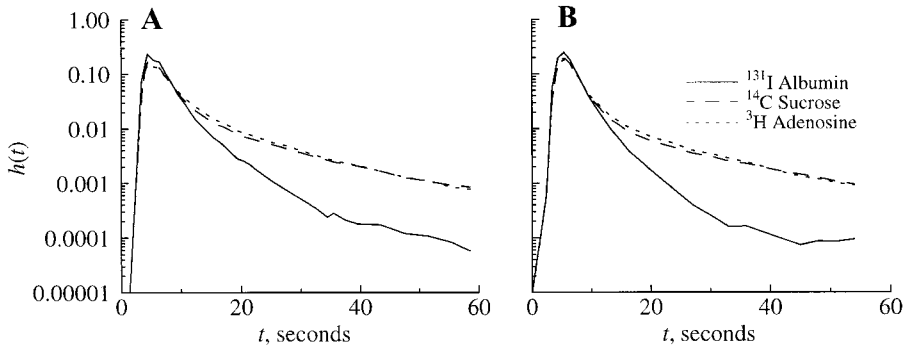

Fig. 2. Inhibition of adenosine transport with dipyridamole and nitrobenzylthioinosine (NBTI). Normalized outflow dilution curves were obtained during perfusion with KRB containing either 20 μM dipyridamole (*A*; *experiment 2107886*) or 5 μM NBTI (*B*; *experiment 1101895*).

adenosine presumably crosses the capillary wall only by permeating the clefts between endothelial cells, as does sucrose, and cannot enter cells. The curves for adenosine and sucrose would not be expected to completely superimpose on each other because of differences in diffusion coefficients and therefore in permeability (PS_g) through the clefts. The presence of blocker in the perfusate prevented significant metabolism of the injected adenosine tracer (Table 1), as would be expected when adenosine transport into the cells is hindered so that access to intracellular sites of metabolism is slowed.

Estimation of K_m and V_{max} for adenosine on the endothelial nucleoside transporter. With the use of the E_{max} data on sucrose and adenosine from Table 1, values for PS_{ecl} were calculated by use of *Eq. 4*. These values of PS_{ecl} are plotted in Fig. 3; the whole set was fitted with the Michaelis-Menten equation (*Eq. 3*) to give by nonlinear least squares a $PS_{ecl\,max}$ of 1.12 $ml \cdot g^{-1} \cdot min^{-1}$, an apparent K_m of 112 ± 12 μM, and a $V_{max}S$ product of 124 $nmol \cdot g^{-1} \cdot min^{-1}$ or a V_{max} of 0.25 ± 0.023 $\mu M \cdot cm \cdot min^{-1}$. The *top line* (dashed) represents *Eq. 3* with the use of V_{max} + 2 SD (=0.272 $\mu M \cdot cm \cdot min^{-1}$) and K_m + 2 SD (=124 μM). Likewise, the dotted line represents −2 SD for both. Thus the dashed and dotted lines enclose a bit more area than the 95% confidence limits because they are drawn for the combination of the upper 95% confidence limits for both K_m and V_{max}.

The cellular retention for adenosine is high, reducing reflux to close to zero, so these are optimal conditions for applying the Crone-Renkin-type analysis. Consequently, under the stated assumptions, one can make an alternative calculation to derive an estimated $\hat{E}_{max}$(Ado) from the transporter parameters, K_m and V_{max}; the adenosine-sucrose permeability ratio, β; and the estimated $PS_g(Suc) = -F \cdot \log_e[1 - E_{max}(Suc)]$. The method takes into account the two parallel routes (cleft and endothelial plasmalemma) for the escape of tracer adenosine from the plasma: from E_{max}(Ado) we calculate PS_T(Ado), as suggested in *Eq. 4*, and we interpret PS_{ecl} as in *Eq. 3*. By doing this, we obtain an estimate of PS_{ecl} and from it an estimate of the expected $\hat{E}_{max}$(Ado); by using the two equations together, we have only the two free parameters, K_m and V_{max}, for optimizing the fit of the estimated $\hat{E}_{max}$ to the observed E_{max}.

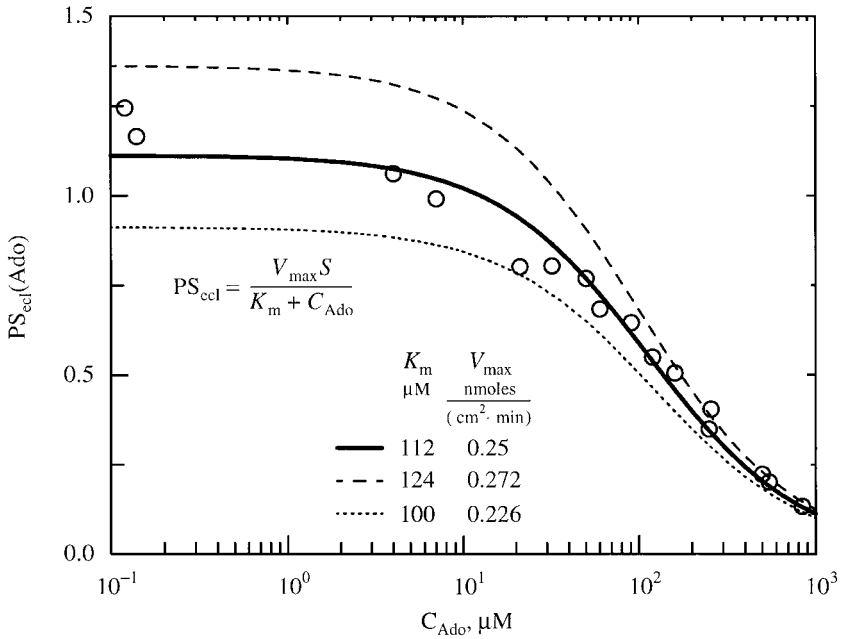

Fig. 3. Estimated permeability (*P*)-surface area (*S*) product via passive transport across the endothelial cell luminal membrane (PS_{ecl}, ○; *from Eq. 4*) for adenosine (Ado) versus venous effluent adenosine concentrations (C_{Ado}). From this, the parameters for the nucleoside transporter on the luminal surface of coronary capillary endothelial cells were estimated by use of nonlinear least squares optimization, assuming Michaelis-Menten kinetics (*Eq. 3*). This gave the Michaelis-Menten constant (K_m) = 112 ± 12 μM, maximum rate of transporter conformational change to move the substrate from one side of the membrane to the other (V_{max}) = 0.25 ± 0.023 $nmol \cdot min^{-1} \cdot cm^{-2}$, and the value for PS_{ecl} when C_{Ado} is zero ($PS_{ecl\,max}$) = 1.12 $ml \cdot g^{-1} \cdot min^{-1}$ for the adenosine transport, where the ± values represent the 95% confidence limits.

Downloaded from ajpheart.physiology.org on June 13, 2009

The results are shown in Fig. 4, with optimization of the transporter parameters K_m and V_{max} with a chosen ratio β for all 16 data sets to fit $\hat{E}_{max}$(Ado) to the observed E_{max}(Ado) from the individual values for E_{max}(Suc), F, and adenosine concentration. With β = 1.2 (from the APPENDIX), the deviations from the line of identity were not systematic and were <2% in E_{max} [correlation coefficient (r) > 0.99]. Figure 4, *top inset*, shows the relationship between the estimated K_m and the value chosen for β. Although the fit between the observed and predicted E_{max} values gave the smallest sum of squared differences where β = 1.24, the sum of squared differences was only 40% larger at the "correct" value of 1.2. With β = 1.2, the estimated K_m was 117 μM, V_{max} = 0.252 μM·cm·min^{-1}, and $V_{max}S$ = 126 nmol·g^{-1}·min^{-1}. The value of V_{max}/K_m was 0.00215 cm/min for β = 1.2. For other choices of β, the "best-fit" values were higher at lower β and vice versa, as shown in Fig. 4, *top inset*. The estimate (uninhibited) for $PS_{ecl\,max}$ was 1.08 ml·g^{-1}·min^{-1} by this analysis, slightly lower than the estimated $PS_{ecl\,max}$ of 1.12 ml·g^{-1}·min^{-1} found by the analysis in Fig. 3.

DISCUSSION

These studies demonstrate that adenosine is transported into guinea pig cardiac capillary endothelial cells by a low-affinity, high-capacity saturable carrier, inhibitable by both NBTI and dipyridamole. With the use of the two methods of analysis, average values for the kinetic parameters of the adenosine transporter on the luminal surface of the endothelial cells are as follows: K_m = ~114 ± 12 μM, V_{max} = 0.25 ± 0.023 μM·cm·min^{-1}, $V_{max}S$ = 125 nmol·g^{-1}·min^{-1}, and PS_{ecl} = 1.1 ml·g^{-1}·min^{-1} on the luminal surface of these cells by use of two methods of analysis.

The multiple-indicator dilution technique, in combination with a model for transcapillary exchange via interendothelial clefts and endothelial cells in parallel, has some advantages for estimating membrane transport kinetics. The simple model analysis enables one to distinguish transport kinetics through the luminal surface of the endothelial cells from permeation through the interendothelial clefts, although it does not give measures of intracellular accumulation and consumption.

Our analysis provides no information on the rates of transport across the abluminal endothelial surface or into parenchymal cells. In previous analyses using a full capillary-endothelial-interstitial space-parenchymal cell model (45, 50), we had learned that abluminal endothelial permeability-surface area product (PS_{eca}) could not be accurately determined. The reason is that the intraendothelial consumption is high, so there is little or no flux of the tracer adenosine across the abluminal surface, and its influence on the outflow dilution curve is therefore essentially unmeasurable. Different experiments need to be done to elicit clear estimates of PS_{eca}; perhaps combinations of blocking intracellular phosphorylation and deamination will prove useful.

In principle, one must question the use of the simple symmetrical first-order Michaelis-Menten model for the description of transport kinetics across a membrane. The approach is adequate when concentrations on the *trans* side of the membrane do not influence the *cis*-to-*trans* flux: this is the symmetry assumption. (There is at least a suspicion of asymmetry for uridine transport in ATP-depleted cells; see Ref. 38.) Whether or not the affinities of adenosine for the carrier are the same on the two sides, the transporter must, after

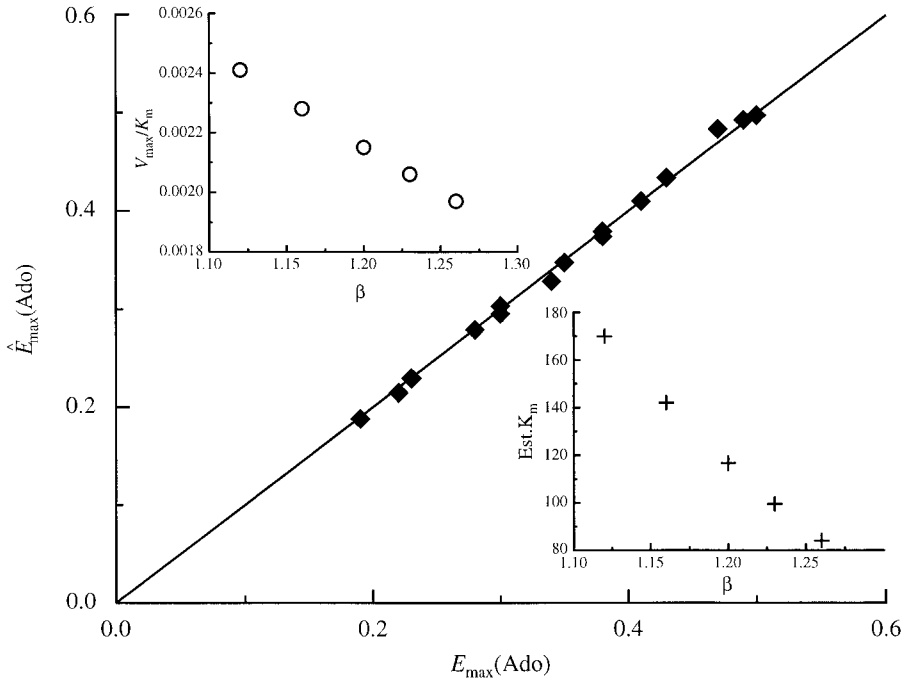

Fig. 4. Estimated adenosine extractions [$\hat{E}_{max}$(Ado)] from single capillary analysis, assuming no back diffusion, versus observed extractions [E_{max}(Ado)] in guinea pig hearts. $\hat{E}_{max}$(Ado) = 1 − exp(−PS_T/F), where PS_T (total apparent permeability-surface area product) = 1.2 PS_g(Suc) + PS_{ecl} (Ado); PS_{ecl} (Ado) = $V_{max}S/(K_m + C_{Ado}$, as in *Eq. 3*. At β (the expected ratio of permeabilities through the interendothelial clefts) = 1.2, K_m = 117 μM and $PS_{ecl\,max}$ = $V_{max}S/K_m$ = 1.08 ml·g^{-1}·min^{-1}. The line is the line of identity. The correlation coefficient (r) > 0.99 (n = 16). *Bottom right inset* (+ symbols): dependency of the apparent (Est) K_m on the choice of β. *Top left inset* (○): dependency of the estimate of V_{max}/K_m on the choice of β.

Downloaded from ajpheart.physiology.org on June 13, 2009

transporting a substrate molecule from the *cis* side to the *trans* side, become reavailable on the *cis* side before it can carry an adenosine molecule from *cis* to *trans*. When the free and complexed forms of the carrier have the same rates of conformational change after flipping the active site from one side to the other (or an equivalent mechanism), the apparent K_m is twice the equilibrium binding or dissociation constant. If the free carrier permeability were infinitely high, then the K_m would equal the equilibrium constant. No blood-tissue exchange model accounting for bidirectional, saturable transport with countertransport has been published at this point, and with the absence of information with respect to countertransport facilitation or inhibition, the working assumption that the transporter kinetics are first-order Michaelis-Menten seems appropriate.

In studies of purine transport into erythrocytes, Schrader et al. (43) and Jarvis (20) found evidence for two transporters with differing affinities for the purine that also had differing affinities for competitive blockers. Using blockers or inhibitors of the transporter, we show in this study that there is no significant adenosine transport across the plasmalemma, either via a second unblocked transporter or by a passive nonfacilitated mechanism. Total inhibition of PS_{ecl} by a single agent eliminates both from consideration.

Mammalian cells almost universally possess a single nonconcentrative nucleoside transport system that exhibits broad nucleoside specificity and similar kinetic properties. All information available at present indicates that adenosine is transported into cells by the same carrier that transports uridine, thymidine, and other ribo- and deoxyribonucleosides. However, the transporters may differ in sensitivity to NBTI and other transport inhibitors in different cell types (36, 37, 51). Adenosine transport in guinea pig endothelial cells and myocytes was almost completely blocked by both NBTI and dipyridamole in concentrations used in this study.

Nucleoside transport has been studied most extensively for uridine and thymidine in human erythrocytes that lack kinases and phosphorylases for uridine and thymidine and in cells in which phosphorylation was blocked by depletion of cells of ATP. Similar studies with adenosine, however, have been complicated by the multitude of enzymes involved in its salvage. Besides being directly phosphorylated, adenosine is rapidly deaminated to inosine, and inosine is rapidly phosphorylyzed to hypoxanthine, which in turn is phosphoribosylated to form inosine monophosphate. Furthermore, all unphosphorylated intermediates are subject to transport out of the cell.

Plagemann et al. (38) examined ATP-depleted human erythrocytes treated with 2′-deoxycoformycin to measure kinetics of equilibrium exchange and zero-trans influx of adenosine in the absence of metabolic conversions. In zero-trans experiments the substrate concentration on the trans (opposite) side of the membrane is virtually zero. Michaelis-Menten parameters for both protocols were estimated at a K_m of 60 μM and a $V_{max}S$ of 25–30 pmol·μl cell water^{-1}·s^{-1} or 1.8 μmol·ml cell water^{-1}·min^{-1} or ~1.2 μmol·g^{-1}·min^{-1}. These values are similar to those reported for adenosine transport in cultured leukemia cells (24, 35, 37). Their $V_{max}S$ products are ~10 times higher than ours. At the other extreme, the uptake of adenosine by dog erythrocytes is almost negligible. Given such wide ranges of possibilities, we cannot generalize from our observations on guinea pig cardiac capillary endothelial cells, but we can safely conclude that these guinea pig endothelial cells are abundantly supplied with purine nucleoside transporters, as recognized by Parkinson and Clanachan (32).

We should comment that in some situations it appears there is active or concentrative transport for purine nucleosides. Concentrative, sodium-dependent, active transport of nucleosides has been found in the cells of the kidney (1, 23), intestinal epithelia (33, 46), and choroid plexus (47, 48) but not in erythrocytes, various tumor cells, hepatocytes, and numerous untransformed and transformed mammalian cell culture lines (34). The active concentrative transport of nucleosides appears unaffected by the recognized inhibitors of the facilitated transport (47). Because cardiac endothelial uptake is blocked by dipyridamole and NBTI, the inference is therefore that the observed transport is facilitated but probably not concentrative.

A question arises when comparing the estimates of the maximum value of PS_{ecl}, which equals $V_{max}S/K_m$, from these experiments with those of previous studies (45, 50). Both of these earlier studies (45, 50) were done without background nontracer adenosine, i.e., tracer only, giving estimates of PS_{ecl} of ~4 and 2 ml·g^{-1}·min^{-1}, whereas the estimates here were ~1.1 ml·g^{-1}·min^{-1}. In this study, the experiments without any background (first two experiments of Table 1) were preceded by studies with high background. That the prior adenosine administration influenced the PS_{ecl} would seem unexpected, because there were many minutes to allow a return to control state. However, this surmise is only partly affirmed by the data showing 120 and 140 nM adenosine in the venous effluent, values substantially above what is anticipated for healthy perfused guinea pig hearts. Another possible explanation is the method of analysis, for here we assumed that E_{max} gave a measure of unidirectional flux, something that we know is not valid for unconsumed tracers. The resolution of this question would seem to lie in undertaking a full nonlinear model analysis; our preliminary efforts in this direction do suggest a possibly higher V_{max} but appear not to affect K_m.

Remembering that species differences are large (8, 45) and that transporter characteristics may vary from species to species and from one cell type to another in the same species, it would be presumptuous to expect our estimates of V_{max} to apply to the other situations. The estimates of K_m have a greater chance of being broadly applicable, because K_m is not dependent on the amount of protein expressed but only on its sequence, folding, membrane insertion, and particular local conditions. The concentration dependency of the endothelial conductances (PS_{ecl}) are important governors of the

Downloaded from ajpheart.physiology.org on June 13, 2009

fate of plasma and interstitial adenosine: PS_{ecl} is high enough and its K_m is so high that at normal physiological levels and even at the levels of adenosine reached during hypoxia, there will be rapid cellular uptake even while there is not adenosine release. At the higher levels found in hypoxia and ischemia, this high conductance will lead to saturation of adenosine kinase (K_m of ~1 μM) and therefore relatively higher rates of deamination (K_m for adenosine deaminase is higher than for the kinase). This system for adenosine transport and metabolism should be analyzed with a fully developed nonlinear systems model representing purine nucleoside degradation and trapping as AMP and inosine 5′-monophosphate.

APPENDIX

Estimation of the ratio β of free diffusion coefficients for adenosine and sucrose. β should, in theory, be not more than 1–2% higher than the ratio of free diffusion coefficients (D_{Ado} and D_{Suc} for adenosine and sucrose, respectively; D_{Ado}/D_{Suc}), given that the cleft widths are 100–150 Å and that the difference in steric hindrances is small, so the primary requirement is to find the ratio of the free diffusion coefficients. Initially we thought that β might be assumed to be 1.12, the reciprocal of the ratio of the square roots of the molecular weights (MW) for sucrose and adenosine, respectively {[MW(Suc)/MW(Ado)]$^{1/2}$ = (342/267.2)$^{1/2}$}, a standard approach (49) to estimating diffusion coefficients from the molecular weights when one of the D values has been measured. However, with β = 1.12, the estimated values of $\hat{E}_{max}$(Ado) varied systematically from the observed E_{max}(Ado), being too high at low adenosine concentration. Empirically, values of β = 1.20–1.26 gave much better overall fits with little systematic bias. With different β values, the best fits gave different estimates of $V_{max}S$ and K_m, but the ratio $V_{max}S/K_m$ was nearly constant at 1.0 ml·g^{-1}·min^{-1}.

This was interesting from the point of view of separability versus interdependence of the estimates. Examination of contour plots of the sum of squares of E_{max} (observed) versus $\hat{E}_{max}$ (estimated) showed that for each β, there was a long, straight, steep-sided valley in the plane defined by K_m and $V_{max}S$. Each valley followed the line $V_{max}S/K_m$ = constant, and each β gave only a slight lateral shift of the valley. The bottoms of the narrow valleys were shallowly sloped, and although the minima were well defined, a 10–20% shift along the valley bottom gave only a slightly worse fit. Moreover, although the valleys at different β values shifted very little laterally, their minima along the valley showed a 20% shift with a 6% change in β. This means that whereas $V_{max}S/K_m$ was narrowly defined, the component terms were not and were strikingly dependent on β.

β is almost a physical constant, and there should be little uncertainty in it, in principle. However, a diffusion coefficient for adenosine in water has not been reported. Diffusion coefficients in water are dependent on molecular size, shape, and charge as well as molecular weight. A general approach to estimating D is to use the effective molecular volumes. Two ways to estimate molecular volumes from atomic volumes have evolved: LeBas volumes and van der Waals volumes (40). They are approximate because they do not account precisely for how tightly the atoms fit together. However, they are both fairly refined and give, for example, empirical reductions in volume to account for ring structures and for different types of bonding. We used the van der Waals volumes recommended by Edward (12) and the LeBas volumes listed by Hayduk and Laudie (17). From the former, β = 1.18; from the latter, β = 1.165.

Another approach is to calculate $\beta = (V_{Suc}/V_{Ado})^{1/3}$, where the volumes (V) for sucrose and adenosine (V_{Suc} and V_{Ado}, respectively) were calculated from the maximal diameters at right angles to each other, as suggested for asymmetric ellipsoids by Schultz and Solomon (44). To obtain the diameters, we used the PROPHET system for molecular design (18) to produce three-dimensional space-filling molecular models, printed these at varied rotations, measured the three orthogonal diameters, and calculated the relative volumes. This gave β = 1.21. We settled on a compromise value of β = 1.20 for use in estimating PS_g(Ado) from PS_g(Suc).

From this, given that the aqueous diffusion coefficient of sucrose (D_{Suc}) in weak electrolyte solutions at 37°C is $0.704 \cdot 10^{-5} \cdot cm^2 \cdot s^{-1}$ (calculated from Table 11.4 and Appendix 1.1 in Ref. 41), then $D_{Ado} = 0.845 \cdot 10^{-5} \cdot cm^2 \cdot s^{-1}$ at 37°C.

We thank Kenneth Applegate for guidance in the use of PROPHET, which is supported by National Institutes of Health/National Center for Research Resources Primate Center Grant 5-P51-RR-00166. The advice of Bruce Graham with respect to the use of LeBas atomic volumes is much appreciated.

The experiments were supported by National Heart, Lung, and Blood Institute (NHLBI) Grant HL-19139. L. M. Schwartz was supported by NHLBI Cardiovascular Bioengineering Training Grant HL-07403.

Programs for the analysis of data like ours are available on the National Simulation Resource website by downloading the simulation interface system, XSIM, and the model programs (http://nsr.bioeng.washington.edu). The data are available by request.

Present addresses: L. M. Schwartz, Physiology Dept., Uniformed Services Univ. of the Health Sciences, 4301 Jones Bridge Rd., Bethesda, MD 20814-4799; T. R. Bukowski, Zymogenetics, 1201 Eastlake Ave. E, Seattle, WA 98102-3702.

REFERENCES

1. **Angielski S, Le Hir M, and Dubach UC.** Transport of adenosine by renal brush border membranes. *Pflügers Arch* 397: 75–77, 1983.
2. **Barker PH and Clanachan AS.** Inhibition of adenosine accumulation into guinea pig ventricle by benzodiazepines. *Eur J Pharmacol* 78: 241–244, 1982.
3. **Bassingthwaighte JB and Beard DA.** Fractal ^{15}O-water washout from the heart. *Circ Res* 77: 1212–1221, 1995.
4. **Bassingthwaighte JB and Goresky CA.** Modeling in the analysis of solute and water exchange in the microvasculature. In: *Handbook of Physiology. The Cardiovascular System. Microcirculation*. Bethesda, MD: Am. Physiol. Soc., 1984, sect. 2, vol. IV, pt. 1, chapt. 13, p. 549–626.
5. **Bassingthwaighte JB, Malone MA, Moffett TC, King RB, Chan IS, Link JM, and Krohn KA.** Molecular and particulate depositions for regional myocardial flows in sheep. *Circ Res* 66: 1328–1344, 1990.
6. **Bassingthwaighte JB, Wang CY, and Chan IS.** Blood-tissue exchange via transport and transformation by endothelial cells. *Circ Res* 65: 997–1020, 1989.
7. **Bassingthwaighte JB, Yipintsoi T, and Harvey RB.** Microvasculature of the dog left ventricular myocardium. *Microvasc Res* 7: 229–249, 1974.
8. **Borgers M and Thone F.** Species differences in adenosine metabolic sites in the heart. *Histochem J* 24: 445–452, 1992.
9. **Bowditch J, Brown AK, and Dow JW.** Accumulation and salvage of adenosine and inosine by isolated mature cardiac myocytes. *Biochim Biophys Acta* 844: 119–128, 1985.
10. **Chan IS, Goldstein AA, and Bassingthwaighte JB.** SENSOP: a derivative-free solver for nonlinear least squares with sensitivity scaling. *Ann Biomed Eng* 21: 621–631, 1993.
11. **Crone C.** The permeability of capillaries in various organs as determined by the use of the "indicator diffusion" method. *Acta Physiol Scand* 58: 292–305, 1963.

Downloaded from ajpheart.physiology.org on June 13, 2009

12. **Edward JT.** Molecular volumes and the Stokes-Einstein equation. *J Chem Ed* 47: 261–270, 1970.
13. **Gonzalez F and Bassingthwaighte JB.** Heterogeneities in regional volumes of distribution and flows in the rabbit heart. *Am J Physiol Heart Circ Physiol* 258: H1012–H1024, 1990.
14. **Gorman MW, Bassingthwaighte JB, Olsson RA, and Sparks HV.** Endothelial cell uptake of adenosine in canine skeletal muscle. *Am J Physiol Heart Circ Physiol* 250: H482–H489, 1986.
15. **Guller B, Yipintsoi T, Orvis AL, and Bassingthwaighte JB.** Myocardial sodium extraction at varied coronary flows in the dog: estimation of capillary permeability by residue and outflow detection. *Circ Res* 37: 359–378, 1975.
16. **Harmsen E, deJong JW, and Seriuys PW.** Hypoxanthine production by ischemic heart demonstrated by pressure liquid chromatography of blood purine nucleosides and oxypurines. *Clin Chim Acta* 115: 73–84, 1981.
17. **Hayduk W and Laudie H.** Prediction of diffusion coefficients for nonelectrolytes in dilute aqueous solutions. *J Am Inst Chem Eng* 20: 611–615, 1974.
18. **Hollister C.** PROPHET: a national computing resource for life science research. *Nucleic Acids Res* 16: 1873–1875, 1988.
19. **Hopkins SV and Goldie RG.** A species difference in the uptake of adenosine by heart. *Biochem Pharmacol* 20: 3359–3365, 1971.
20. **Jarvis SM.** Kinetic and molecular properties of nucleoside transporters in animal cells. In: *Topics and Perspectives in Adenosine Research*, edited by Gerlach E and Becker BF. Berlin: Springer-Verlag, 1987, p. 102–117.
21. **King RB, Raymond GM, and Bassingthwaighte JB.** Modeling blood flow heterogeneity. *Ann Biomed Eng* 24: 352–372, 1996.
22. **Kuikka J, Levin M, and Bassingthwaighte JB.** Multiple tracer dilution estimates of D- and 2-deoxy-D-glucose uptake by the heart. *Am J Physiol Heart Circ Physiol* 250: H29–H42, 1986.
23. **Le Hir ML and Dubach UC.** Sodium gradient-energized concentrative transport of adenosine in renal brush border vesicles. *Pflügers Arch* 401: 58–63, 1984.
24. **Lum CT, Marz R, Plagemann PGW, and Wohlheuter RM.** Adenosine transport and metabolism in mouse leukemia cells and in canine thymocytes and peripheral blood leukocytes. *J Cell Physiol* 101: 173–200, 1979.
25. **Manfredi JP and Sparks HV Jr.** Adenosine's role in coronary vasodilation induced by atrial pacing and norepinephrine. *Am J Physiol Heart Circ Physiol* 243: H536–H545, 1982.
26. **McConahey PJ and Dixon FJ.** A method of trace iodination of proteins for immunologic studies. *Int Arch Allergy Appl Immunol* 29: 185–189, 1966.
27. **Meghji P, Holmquist CA, and Newby AC.** Adenosine formation and release from neonatal-rat heart cells in culture. *Biochem J* 229: 799–805, 1985.
28. **Moffett TC, Chan IS, and Bassingthwaighte JB.** Myocardial serotonin exchange: negligible uptake by capillary endothelium. *Am J Physiol Heart Circ Physiol* 254: H570–H577, 1988.
29. **Mustafa SJ.** Effects of coronary vasodilator drugs on the uptake and release of adenosine in cardiac cells. *Biochem Pharmacol* 28: 2617–2624, 1979.
30. **Olsson RA and Pearson JD.** Cardiovascular purinoceptors. *Physiol Rev* 70: 761–845, 1990.
31. **Olsson RA, Snow JA, Gentry MK, and Frick GP.** Adenosine uptake by canine heart. *Circ Res* 31: 767–778, 1972.
32. **Parkinson FE and Clanachan AS.** Adenosine receptors and nucleoside transport sites in cardiac cells. *Br J Pharmacol* 104: 399–405, 1991.
33. **Paterson ARP, Jakobs ES, Ng CYC, Odegard RD, and Adjei AA.** Nucleoside transport inhibition in vitro and in vivo. In: *Topics and Perspectives in Adenosine Research. Proceedings of the 3rd International Symposium on Adenosine Munich 1986*, edited by Gerlach E and Becker BF. Berlin: Springer-Verlag, 1987, p. 89–101.
34. **Plagemann PGW and Wohlhueter RM.** Permeation of nucleosides, nucleic acid bases, and nucleotides in animal cells. *Curr Top Membr Transp* 14: 225–330, 1980.
35. **Plagemann PGW and Wohlhueter RM.** Nucleoside transport in mammalian cells and interaction with intracellular metabolism. In: *Regulatory Function of Adenosine*, edited by Berne RM, Rall TW, and Rubio R. The Hague, The Netherlands: Martinus Nijhoff, 1983, p. 179–201.
36. **Plagemann PGW and Wohlhueter RM.** Kinetics of nucleoside transport in human erythrocytes: alterations during blood preservation. *Biochim Biophys Acta* 778: 176–184, 1984.
37. **Plagemann PGW and Wohlhueter RM.** Effects of nucleoside transport inhibitors on the salvage and toxicity of adenosine and deoxyadenosine in L1210 and P338 mouse leukemia cells. *Cancer Res* 45: 6418–6424, 1985.
38. **Plagemann PGW, Wohlhueter RM, and Kraupp M.** Adenine nucleotide metabolism and nucleoside transport in human erythrocytes under ATP depletion conditions. *Biochim Biophys Acta* 817: 51–60, 1985.
39. **Prinzen FW and Bassingthwaighte JB.** Blood flow distributions by microsphere deposition methods. *Cardiovasc Res* 45: 13–21, 2000.
40. **Reid RC, Prausnitz JM, and Sherwood TK.** *The Properties of Gases and Liquids*. New York: McGraw-Hill, 1977.
41. **Robinson RA and Stokes RH.** *Electrolyte Solutions* (2nd ed.). London: Butterworths, 1959.
42. **Schrader J.** Metabolism of adenosine and sites of production in the heart. In: *Regulatory Function of Adenosine*, edited by Berne RM, Rall TW, and Rubio R. The Hague, The Netherlands: Nijhoff, 1983, p. 133–156.
43. **Schrader J, Berne RM, and Rubio R.** Uptake and metabolism of adenosine by human erythrocyte ghosts. *Am J Physiol* 223: 159–166, 1972.
44. **Schultz SG and Solomon AK.** Determination of the effective hydrodynamic radii of small molecules by viscometry. *J Gen Physiol* 44: 1189–1199, 1961.
45. **Schwartz LM, Bukowski TM, Revkin JH, and Bassingthwaighte JB.** Cardiac endothelial transport and metabolism of adenosine and inosine. *Am J Physiol Heart Circ Physiol* 277: H1241–H1251, 1999.
46. **Schwenk M, Hegazy E, and del Pino VL.** Uridine uptake by isolated intestinal epithelial cells of guinea pig. *Biochim Biophys Acta* 805: 370–374, 1984.
47. **Spector R.** Thymidine transport and metabolism in choroid plexus: effect of diazepam and thiopental. *J Pharmacol Exp Ther* 235: 16–19, 1985.
48. **Spector R and Huntoon S.** Specificity and sodium dependence of the active nucleoside transport system in choroid plexus. *J Neurochem* 42: 1048–1052, 1984.
49. **Stein WD.** *Transport and Diffusion Across Cell Membranes*. Orlando, FL: Academic, 1986.
50. **Wangler RD, Gorman MW, Wang CY, DeWitt DF, Chan IS, Bassingthwaighte JB, and Sparks HV.** Transcapillary adenosine transport and interstitial adenosine concentration in guinea pig hearts. *Am J Physiol Heart Circ Physiol* 257: H89–H106, 1989.
51. **Williams EF, Barker PH, and Clanachan AS.** Nucleoside transport in heart: species differences in nitrobenzylthioinosine binding, adenosine accumulation, and drug-induced potentiation of adenosine action. *Can J Physiol Pharmacol* 62: 31–37, 1984.
52. **Zimmer HG, Trendelenburg C, Kammermeier H, and Gerlach E.** De novo synthesis of myocardial adenine nucleotides in the rat. *Circ Res* 32: 635–642, 1973.

Downloaded from ajpheart.physiology.org on June 13, 2009